Fibers and Polymers 2003, Vol.4, No.2, 89-96

Injection Molding of Vertebral Fixed Cage Implant

Kyung Min Yoo, Seok Won Lee, Jae Ryoun Youn*, Do Heum Yoon[1], Yong Eun Cho[1], Jae-Pil Yu[2], and Hyung Sang Park[2]

School of Materials Science and Engineering, Seoul National University, Seoul 151-742, Korea
[1]Department of Neurosurgery, College of Medicine, Yonsei University, Seoul 120-749, Korea
[2]Kyungwon Medical Company, 718-19, Jeil Bldg., Yoksam-dong, Seoul 135-924, Korea
(Received April 12, 2003; Revised May 20, 2003; Accepted May 28, 2003)

Abstract: A vertebral cage is a hollow medical device which is used in spine surgery. By implanting the cage into the spine column, it is possible to restore disc and relieve pressure on the nerve roots. Most cages have been made of titanium alloys but they detract the biocompatibility. Currently PEEK (polyether ether ketone) is applied to various implants because it has good properties like heat resistance, chemical resistance, strength, and especially biocompatibility. A new shape of vertebral cage is designed and injection molding of PEEK is considered for production. Before injection molding of the cage, it is needed to evaluate process conditions and properties of the final product. Variables affecting the shrinkage of the cage are considered, e.g., injection time, packing pressure, mold temperature, and melt temperature. By using the numerical simulation program, MOLDFLOW, several cases are studied. Data files obtained by MOLDFLOW analysis are used for stress analysis with ABAQUS, and shrinkage and residual stress fields are predicted. With these results, optimum process conditions are determined.

Keywords: Vertebral cage, Injection molding, Numerical simulation, Shrinkage, Residual stress

Introduction

In recent years the excitement about the development and use of spine cage[1,2] has escalated. The cage is a small hollow cylindrical device and usually made of titanium alloys because the titanium alloy makes it very strong and durable. The shape of cage commercially available being used in the surgery is shown in Figure 1. The lumbar vertebrae are the bones of the spinal column. These bones are separated from each other by the lumbar disc, which acts as a shock absorber. When a disc is damaged, the vertebrae grate against each other during motion and cause nerve impingement. The purpose of using cages is often to restore disc height which has been reduced from a collapsed disc and to relieve pressure on nerve roots. A cage can eliminate the grating motion, increase the space for the nerve roots, stabilize the spine, restore spine alignment, and relieve the severe pain. Patients who have undergone surgery have cages implanted between two vertebrae. When the hollow space inside the cage has been neatly packed by bone debris, bone tissues begin to grow through the fusion area[1] of the cages eventually forming a solid bond holding the two vertebrae together.

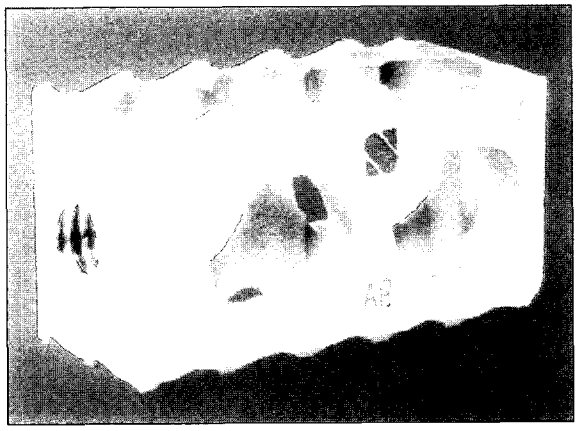

Figure 1. Shape of the commercially available cage.

*Corresponding author: jaeryoun@snu.ac.kr

In recent years, cages have undergone numerous modifications to improve their effectiveness. Especially people are trying to find a new material, which can replace titanium. Because cages made of titanium detract the biocompatibility, attention is focused on PEEK (polyether ether ketone). It has good properties like heat resistance, chemical resistance, strength, and especially biocompatibility.

In this study, a new vertebral cage is designed and various conditions of injection molding are evaluated by using commercial codes, I-DEAS, MOLDFLOW, and ABAQUS. Optimal process conditions are found when PEEK is used for injection molding[3-25]. Maintaining the dimensional accuracy of the final part is critical for medical applications, and dimensional accuracy is regarded as the most important factor when the optimal process condition is decided. The residual stress distribution in the body of cage is also predicted to determine the optimum condition.

Numerical Simulation

Constitutive Equations

For the numerical analysis, a general compressible Hele-

Shaw model is used to deal with compressibility of fluid during injection molding.

$$G\frac{\partial p}{\partial t} - \frac{\partial}{\partial x}\left(\tilde{S}\frac{\partial p}{\partial x}\right) - \frac{\partial}{\partial y}\left(\tilde{S}\frac{\partial p}{\partial y}\right) = -F \tag{1}$$

$$\rho C_p\left(\frac{\partial T}{\partial t} + u\frac{\partial T}{\partial x} + v\frac{\partial T}{\partial y}\right) = k\frac{\partial^2 T}{\partial z^2} + \eta\dot{\gamma}^2 \tag{2}$$

where $\tilde{S} \equiv \int_0^h \rho \int_z^h \frac{\tilde{z}}{\eta} dz$ (3)

$$G = \int_0^\chi \left(\frac{\partial \rho_l}{\partial p}\right)_T dz + \int_\chi^h \left(\frac{\partial \rho_s}{\partial p}\right)_T dz \tag{4}$$

$$F = \int_0^\chi \left(\frac{\partial \rho_l}{\partial T}\right)_p \frac{\partial T}{\partial t} dz + \int_\chi^h \left(\frac{\partial \rho_s}{\partial T}\right)_p \frac{\partial T}{\partial t} dz + (\rho_l - \rho_s)_{z=\chi}\frac{\partial \chi}{\partial t} \tag{5}$$

where x, y, and z are the Cartesian coordinates, u and v are velocity components, p is pressure, T is temperature, ρ is density, C_p is heat capacity, k is thermal conductivity, η is viscosity, χ is the location of the interface, and the subscripts l and s denote liquid and solid phases, respectively. Boundary conditions for the equations are given as follows: zero pressure at the melt front, impermeable condition at the wall of the mold, and constant volume flow rate at the gate. To describe the shear thinning effect, the modified Cross-type model is employed by using the following equation.

$$\eta(\dot{\gamma}, T, p) = \frac{\eta_0(T, p)}{1 + \left(\frac{\eta_0 \dot{\gamma}}{\tau^*}\right)^{1-n}} \tag{6}$$

A WLF-type equation can represent the effect of temperature on the viscosity as follows.

$$\eta_0(T, p) = D_1 \exp\left[-\frac{A_1(T - T^*)}{A_2 + D_3 p + (T - T^*)}\right] \tag{7}$$

$$T^* = D_2 + D_3 p \tag{8}$$

The model parameters for PEEK are tabulated in Table 1.

The Tait state equation is employed to predict the change of density with respect to pressure and temperature.

Table 1. Parameters for the modified Cross model

Symbol	Value
n	0.6342
τ^*	3988.79 Pa
D_1	8.98735×10^{11}
D_2	403.15 K
D_3	0
A_1	24.665
A_2	51.6 K

$$v(T, p) = \frac{1}{\rho(T, p)} = v_0(T)\left[1 - C\ln\left(1 + \frac{p}{B(T)}\right)\right] \tag{9}$$

$$\text{where } v_0(T) = \begin{cases} b_{1,l} + b_{2,l}\bar{T} & (T > T_t) \\ b_{1,s} + b_{2,s}\bar{T} & (T < T_t) \end{cases} \tag{10}$$

$$B(T) = \begin{cases} b_{3,l}\exp(-b_{4,l}\bar{T}) & (T > T_t) \\ b_{3,s}\exp(-b_{4,s}\bar{T}) & (T < T_t) \end{cases} \tag{11}$$

$$\bar{T} = T - b_5 \tag{12}$$

$$T_t(p) = b_5 + b_6 p \tag{13}$$

It is appropriate to introduce an additional term in order to handle the sharp density change in the vicinity of T_t for the case of semicrystalline polymers.

$$v(T, p) = v_0(T)\left[1 - C\ln\left(1 + \frac{p}{B(T)}\right)\right] + v_t(T, p) \tag{14}$$

$$\text{where } v_t(T, p) = \begin{cases} 0 & (T > T_t) \\ b_7 exp(b_8\bar{T} - b_9 p) & (T < T_t) \end{cases} \tag{15}$$

The model constants for PEEK are given in Table 2.

Residual Stress Analysis

A material is called ideally elastic when a deformed body recovers its original shape completely upon removal of the forces causing the deformation and there is a one-to-one relationship between the state of stress and the state of strain for given temperature. Coefficients of the constitutive equation for elastic material depend on temperature. Even though the variation of the elastic constants with temperature is neglected, it is necessary to take account of the thermal expansion, which often produces dimensional changes as large as those caused by the applied forces. When the material is elastically isotropic, the classical elastic constitutive equation, often called the generalized Hooke's law, is expressed as below[26].

Table 2. Parameters for the modified Tait equation

Symbol	Value
$b_{1,l}$	0.0008978 m^3/kg
$b_{2,l}$	6.088×10^{-7} $m^3/kg \cdot K$
$b_{3,l}$	9.7294×10^{-7} Pa
$b_{4,l}$	4.362×10^{-3} K^{-1}
$b_{1,s}$	0.0008198 m^3/kg
$b_{2,s}$	1.763×10^{-7} $m^3/kg \cdot K$
$b_{3,s}$	1.5339×10^{8} Pa
$b_{4,s}$	4.2×10^{-3} K^{-1}
b_5	612.65 K
b_6	1.47×10^{-7} K/Pa
b_7	6.218×10^{-5} m^3/kg
b_8	0.02651 K^{-1}
b_9	4.156×10^{-9} Pa^{-1}

$$T_{ij} = \lambda E_{kk}\delta_{ij} + 2\mu E_{ij} \tag{16}$$

where T_{ij} is Cauchy stress, E_{ij} is small strain, λ and μ are the Lame's elastic constants and δ_{ij} is Kronecker delta. Equation (16) is expressed by introducing ν, Poisson's ratio.

$$E_{ij} = -\frac{\nu}{E}T_{kk}\delta_{ij} + \frac{1+\nu}{E}T_{ij} \tag{17}$$

When the linear thermal stress is induced, equation (16) is expressed as below and equation (17) is also expressed as equation (19).

$$T_{ij} = \lambda E_{kk}\delta_{ij} + 2GE_{ij} - \beta(\theta - \theta_0)\delta_{ij} \tag{18}$$

where G is shear modulus, α and β are thermal expansion coefficients, $(\theta - \theta_0)$ is temperature change.

$$E_{ij} = -\frac{\nu}{E}T_{kk}\delta_{ij} + \frac{1+\nu}{E}T_{ij} + \alpha(\theta - \theta_0)\delta_{ij} \tag{19}$$

$$\beta = \frac{E\alpha}{1-2\nu} = (3\lambda + 2G)\alpha = 3\alpha K \tag{20}$$

where K is the bulk modulus.

Shrinkage Analysis

After cooling, when the injection molded part in the cavity is ejected from the mold, it undergoes warpage[10] caused by the residual stress[21-25] and additional shrinkage is caused by temperature change to room temperature. At ejection, the molded part has the temperature profile along thickness direction. The temperature profile will be changed until uniform temperature is achieved at the room temperature. In this study, it is assumed that the polymer behaves as a linear elastic material. The constitutive equations of a linear elastic body are represented by the following.

$$\sigma_{ij} = E_{ijkl}\varepsilon_{kl} - \beta_{ij}(T - T_0) + (\sigma_r)_{ij} \tag{21}$$

where σ_{ij} is the residual stress calculated in parts and β_{ij} is the material tensor related to thermal expansion coefficient.

$$\beta_{ij} = K\alpha\delta_{ij} \tag{22}$$

The compliance tensor E of the isotropic material is expressed by

$$E_{ijkl} = \frac{2\nu}{(1-2\nu)}G\delta_{ij}\delta_{kl} + G(\delta_{ik}\delta_{jl} + \delta_{il}\delta_{jk}) \tag{23}$$

where ν is Poisson's ratio and G is shear modulus of the material. Material properties of PEEK are listed in Table 3.

Design of the Cage

Two types of a new cage are designed by using a commercial CAD program, I-DEAS. In designing the shape of the vertebral cage, there are some requirements to be met. To make the implant inserted into the fusion area, the front end should be round. Secondly, it should have windows in every face except front face in order to increase the fusion area between the powdered bone and the vertebra. The implant must be strong enough to withstand the compressive force which is known to be around 8000 N. While fusion area becomes larger, it results in thinner walls, and it cannot endure the applied compressive force. So it is important to decide the optimum window size. In order to prevent the powdered bone in the cage from draining, a protective panel is added. Rugged surfaces are applied at the top and bottom

Table 3. Material properties of PEEK

Material data	Symbol	Value
Elastic modulus	E	3500 MPa
Poisson ratio	ν	0.4
Shear modulus	G	1300 MPa
Coefficient of thermal expansion	α	4.9×10^{-5} 1/C
Glass transition temperature	T_g	143 °C
Melt temperature	T_m	343 °C

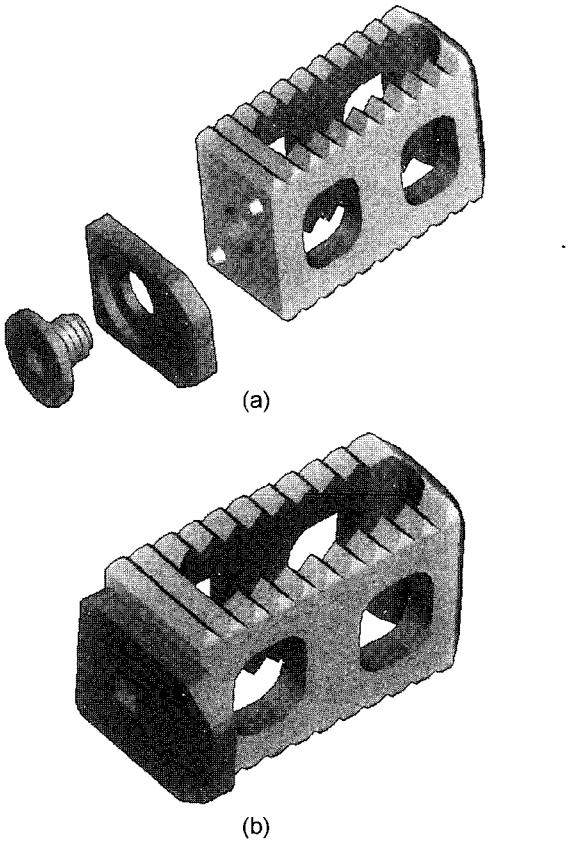

Figure 2. (a) Screw, panel, and cage body before assembly, (b) Screw, panel, and cage body after assembly.

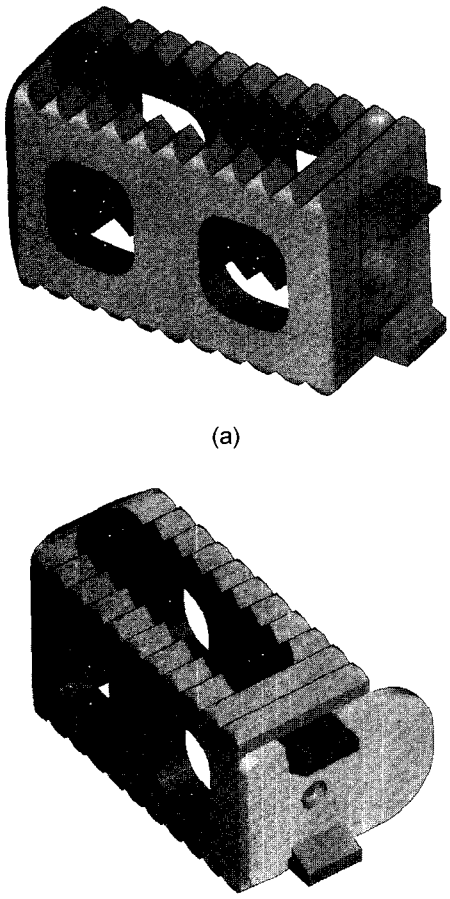

Figure 3. (a) Vertebral PEEK cage body with hooks, (b) Thin panel and click-type cage body after assembly.

faces to prevent the cage from slipping.

To attach the protective panel to the cage, two types are proposed. The first one is shown in Figure 2 before and after the assembly. A tapped hole in the back face is used to fix the panel by a screw. The dimension is $10 \times 12 \times 24$ mm^3. The second type has hooks at the back face to attach the panel as shown in Figure 3. Configurations before and after the assembly are shown in the figure. The dimension is the same as that of the first shape.

Injection Molding Simulation

Shape of the vertebral cage is designed by using I-DEAS and stored as a STL (stereolithography) file for MOLDFLOW analysis. The midplane module consisting of a web of 3-noded triangular elements is employed to create two dimensional mesh as shown in Figure 4. It is generally assumed that the polymer melt flows in plane direction because thickness of the injected part is relatively small. For the mesh shown in Figure 4, 3584 nodes and 6742 triangular elements are used. The cooling lines, gates and runners are designed with the dimensions listed in Table 4. Filling, packing, coolng, and warp are solved with properties of PEEK 151G (Victrex, USA). In order to choose the optimum process conditions, important conditions affecting injection molding are considered, i.e., injection time, packing pressure, mold temperature, and melt temperature. Table 5 lists molding conditions selected for injection molding simulation with MOLDFLOW.

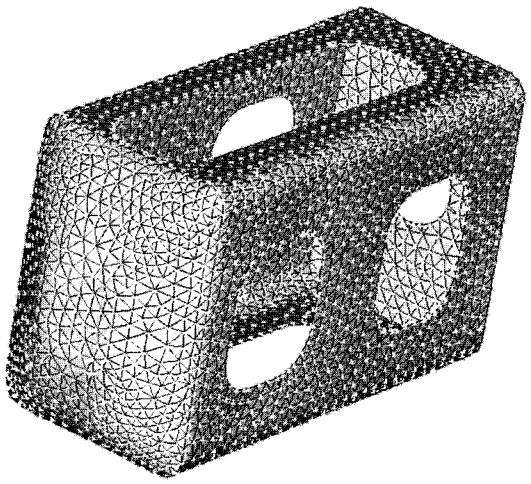

Figure 4. Finite element mesh for the vertebral cage created by the midplane module of MOLDFLOW.

Table 4. Design of runners and cooling lines for the mold

	Diameter (mm)	Length (mm)
Cooling line	8	130
Cold runner 1	3.5-6 (tapered)	70
Cold runner 2	5	40
Cold runner 3	4-4.5 (tapered)	4
Gate	1.2-2 (tapered)	4

Table 5. Simulation conditions selected for the analysis

Case	Injection time (sec)	Mold temperature (°C)	Melt temperature (°C)	Packing pressure (MPa)
1	0.3	185	400	30-20
2	0.5	185	400	30-20
3	0.8	185	400	30-20
4	0.5	185	400	55-30
5	0.5	185	400	80-50
6	0.8	185	400	55-30
7	0.8	185	400	80-50
8	0.8	185	360	30-20
9	0.8	185	440	30-20
10	0.8	205	400	30-20
11	0.8	225	400	30-20

Prediction of Residual Stresses

The molded cage will be implanted into human body during surgery and have to withstand the applied force. The residual stress in the molded part may affect the strength of the cage. Residual stress distribution is calculated assuming that the cage is cooled down to room temperature. Equivalent stress distribution is calculated using the commercial program, ABAQUS (version 6-2). Mises equivalent stress is defined as

$$q = \sqrt{\frac{2}{3}\boldsymbol{S}:\boldsymbol{S}} \tag{24}$$

$$\boldsymbol{S} = \boldsymbol{\sigma} + p\boldsymbol{I} \tag{25}$$

where q is the equivalent stress, $\boldsymbol{\sigma}$ is the stress tensor, p is the equivalent pressure stress, and $\boldsymbol{I}$ is a unit tensor. The input files are obtained from the result of MOLDFLOW. Residual stresses are calculated at different layers, i.e., upper, middle, and lower planes.

Results and Discussion

Shrinkage is determined from the numerical simulation because the dimensional accuracy is one of the most important factors in deciding the optimum process conditions. The magnitude of shrinkage is defined as follows.

$$S\ (\%) = \frac{d_0 - d_1}{d_0} \times 100 \tag{26}$$

where d_0 is the dimension (length, width, height) of the cage designed and d_1 is the dimension of the molded part after cooled to room temperature. The Mises stress distribution obtained by the thermal stress analysis is also described for each case.

Effect of Injection Time

Injection time is varied and the other conditions are fixed in cases 1, 2, and 3 to observe the effect of the injection time.

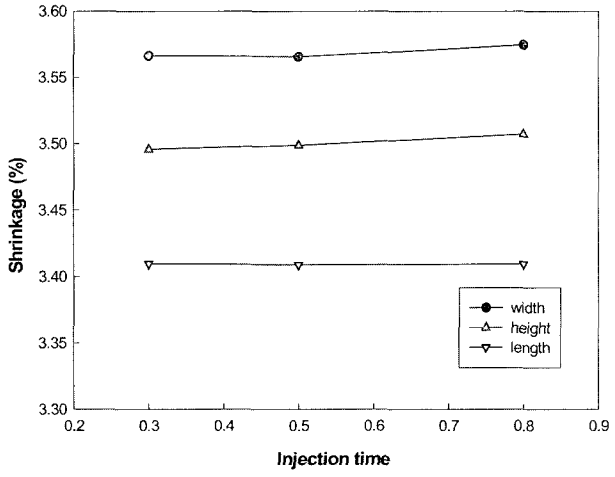

Figure 5. Shrinkage variation with respect to injection time.

The shrinkage variation is shown in Figure 5 and the residual stress is plotted in Figure 6. The shrinkage in width direction is larger than those in other directions. It is found that the injection time has insignificant effect on the shrinkage. According to Figure 6, as the injection time increases, the maximum residual stress is slightly reduced and the residual stresses in between the wall and the center are increased.

Effect of Packing Pressure

Packing pressure is varied for fixed injection time to observe the effect of packing pressure on the shrinkage of the vertebral cage. For two different injection times of 0.5 and 0.8 seconds, the shrinkage is declined and the residual stress is increased as the packing pressure is increased. Because material is compressed during packing stages,

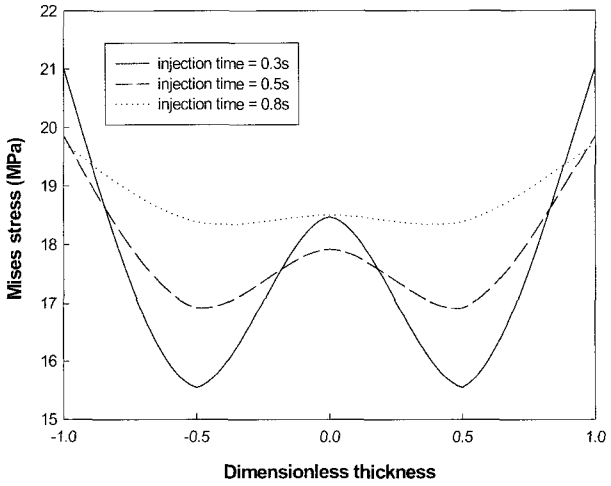

Figure 6. Prediction of residual stress distribution for different injection time.

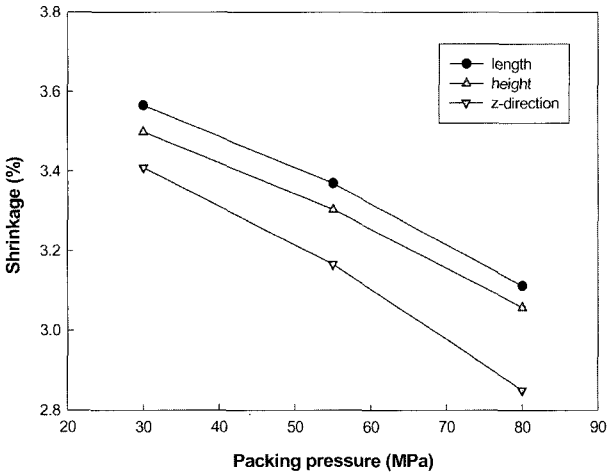

Figure 7. Shrinkage variation with respect to different packing pressure (injection time = 0.5 sec).

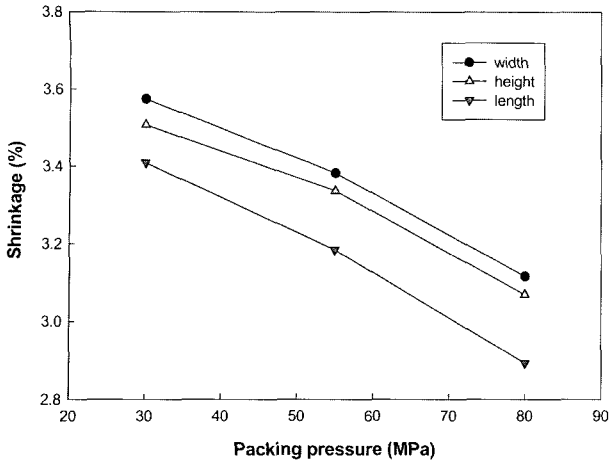

Figure 8. Shrinkage variation with respect to different packing pressure (injection time = 0.8 sec).

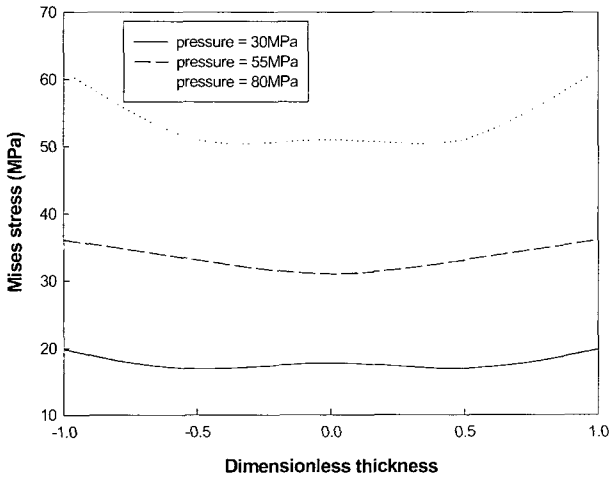

Figure 9. Prediction of residual stress distribution for different packing pressure (injection time = 0.5 sec).

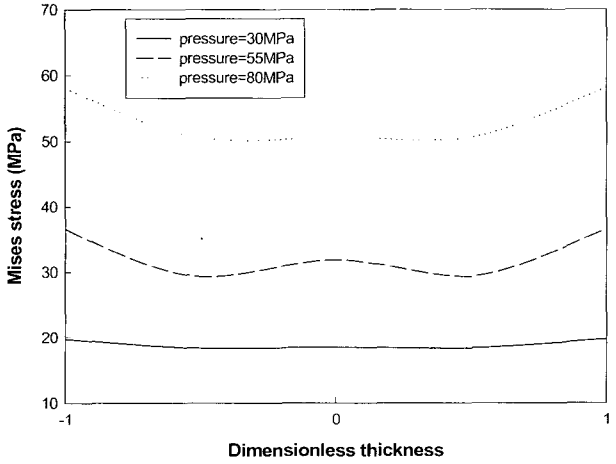

Figure 10. Prediction of residual stress distribution for different packing pressure (injection time = 0.8 sec).

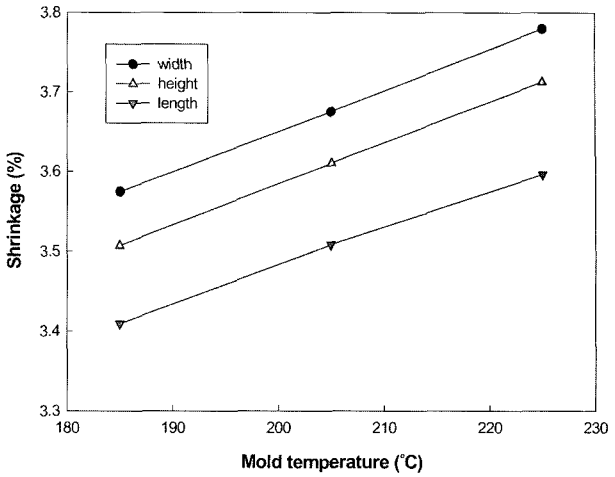

Figure 11. Shrinkage variation with respect to different mold temperature.

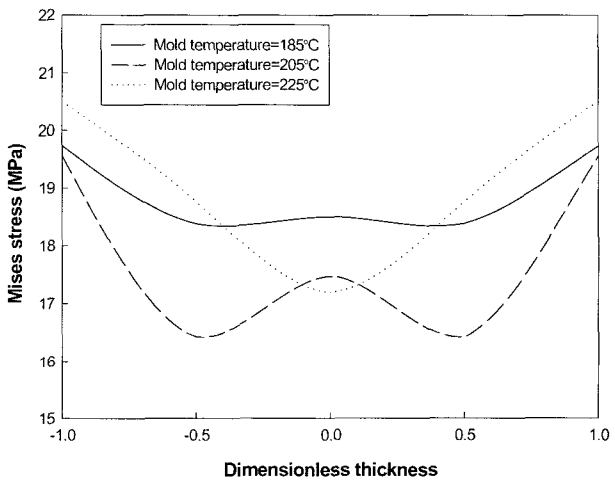

Figure 12. Prediction of residual stress distribution for different mold temperature.

higher packing pressure reduces shrinkage. The shrinkages are shown in Figures 7 and 8 when injection times are 0.5 second and 0.8 second. The residual stress profiles are shown for different packing pressures in Figures 9 and 10.

Effect of Mold Temperature

Mold temperature is varied to identify its effect on the shrinkage of the cage. Shrinkage is shown as a function of mold temperature in Figure 11 and the residual stress profiles are plotted in Figure 12. It is observed that the shrinkage is increased as the mold temperature is increased as shown in Figure 11. Increase of the mold temperature will result in increase of thermal shrinkage after ejection. The residual stress profiles are shown in Figure 12. The residual stress becomes lower at the center of the part as the mold temperature is increased.

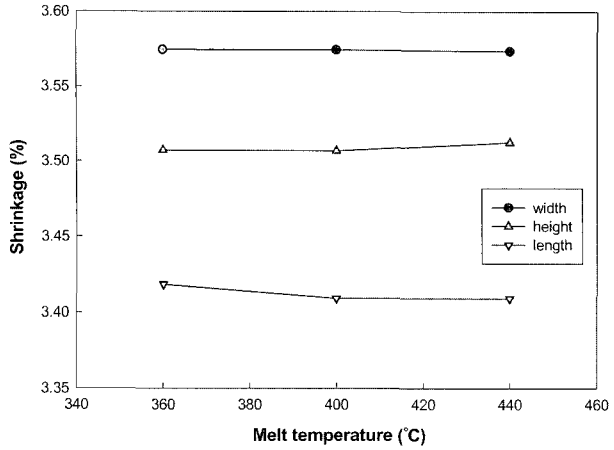

Figure 13. Shrinkage variation with respect to different melt temperature.

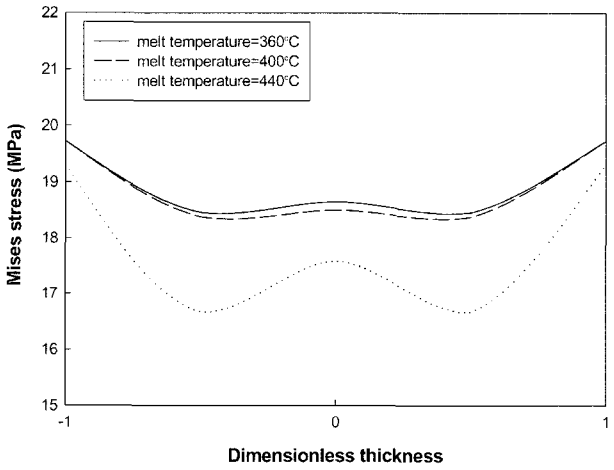

Figure 14. Prediction of residual stress distribution for different melt temperature.

Effect of Melt Temperature

Effect of the mold temperature on the shrinkage is also predicted. Figure 13 shows that the increase of melt temperature reduces the shrinkage slightly because more material can be compressed during packing. The residual stress distribution is also shown in Figure 14. The residual stress is increased as the melt temperature is raised.

From the numerical simulation results, optimum processing conditions are determined for injection molding of the vertebral cage as below; injection time: 0.8 second, packing pressure: 80 MPa, mold temperature: 185 °C, melt temperature: 440 °C.

Conclusions

A vertebral cage is designed for injection molding with PEEK. In order to decide the optimum processing conditions, temperature and pressure profiles, residual stress distributions, and final shrinkage of the part is predicted by using MOLDFLOW and ABAQUS. Processing conditions as mold temperature, melt temperature, packing pressure, and injection time are varied for simulation of injection molding. As the result of numerical simulation, residual stress distribution and deformation of the part are predicted. The optimum molding conditions that can minimize shrinkage and residual stresses are determined from the simulation.

Acknowledgement

This study was supported by the Ministry of Health and Welfare through the venture technology development program (02-PJ1-PG11-VN01-SV03-0016). The authors are grateful for the support.

References

1. C. D. Ray, *Neurosurgery Quarterly*, **7**, 125 (1997).
2. J. W. Brantigan and K. Warden, *Spine*, **18**, 1213 (1993).
3. S. Middleman, "Fundamentals of Polymer Processing", McGraw-Hill, New York, 1977.
4. J. M. Mckelvey, "Polymer Processing", John Wiley and Sons, New York, 1962.
5. Z. Tadmor and C. G. Gogos, "Principles of Polymer Processing", John Wiley and Sons, New York, 1980.
6. H. H. Chiang, C. A. Hieber, and K. K. Wang, *Polym. Eng. Sci.*, **31**, 116 (1991).
7. H. H. Chiang, C. A. Hieber, and K. K. Wang, *Polym. Eng. Sci.*, **31**, 125 (1991).
8. J. Ko and J. R. Youn, *Polym. Compos.*, **16**, 114 (1995).
9. V. Leo and C. Cuvellifz, *Polym. Eng. Sci.*, **36**, 1961 (1996).
10. M. Akay and S. Ozden, *Polym. Eng. Sci.*, **36**, 1839 (1996).
11. K. Shlesh-Nezhad and E. Siores, *J. Mater. Process. Tech.*, **63**, 458 (1997).
12. S. C. Lee, D. Y. Yang, J. Ko, and J. R. Youn, *J. Mater. Process. Tech.*, **70**, 83 (1997).
13. V. W. S. Yung and K. H. Lau, *J. Mater. Process. Tech.*, **63**, 481 (1997).
14. S. C. Lee and J. R. Youn, *J. Reinf. Plast. Comp.*, **18**, 186 (1999).
15. J. H. Jung, S. W. Lee, and J. R. Youn, *Macromol. Symp.*, **148**, 263 (1999).
16. S. W. Lee and J. R. Youn, *Macromol. Symp.*, **148**, 211 (1999).
17. D. Choi and Y. Im, *Compos. Struct.*, **47**, 655 (1999).
18. D. H. Chung and T. H. Kwon, *Korea-Australia Rheology J.*, **12**, 125 (2000).
19. S. W. Lee, J. R. Youn, and J. C Hyun, *Mater. Res. Innov.*, **6**, 189 (2002).
20. K. S. Lee, S. W. Lee, K. Chung, T. J. Kang, and J. R. Youn, *J. Appl. Polym. Sci.*, **88**, 500 (2003).
21. K. M. B. Jansen and G. Titomanlio, *Polym. Eng. Sci.*, **38**,

254 (1998).
22. W. F. Zoetelief and J. Ingenhousz, *Polym. Eng. Sci.*, **36**, 1886 (1996).
23. Y. I. Kwon, T. J. Kang, K. Chung, and J. R. Youn, *Fiber. Polym.*, **2**, 203 (2001).
24. S. K. Kim. S. W. Lee. and J. R. Youn. *Korea-Australia Rheology J.*, **14**, 107 (2002).
25. K. K. Kabenami and H. Wang, *Polym. Eng. Sci.*, **38**, 21 (1998).
26. L. E. Malvern, "Introduction to the Mechanics of a Continuous Medium", Prentice-Hall, Englewood Cliff, 1969.